



## Letter

**Cite this article:** Bradley AT, De Rydt J, Bett DT, Dutrieux P, Holland PR (2022). The ice dynamic and melting response of Pine Island Ice Shelf to calving. *Annals of Glaciology* 63(87-89), 111–115. <https://doi.org/10.1017/aog.2023.24>

Received: 31 October 2022

Revised: 19 January 2023

Accepted: 20 March 2023

First published online: 20 April 2023

**Keywords:**

Calving; ice/ocean interactions; ice shelves; ice-sheet modelling; polar and subpolar oceans

**Corresponding author:**

Alexander T. Bradley; Email: [aleey@bas.ac.uk](mailto:aleey@bas.ac.uk)

# The ice dynamic and melting response of Pine Island Ice Shelf to calving

Alexander T. Bradley<sup>1</sup> , Jan De Rydt<sup>2</sup> , David T. Bett<sup>1</sup>, Pierre Dutrieux<sup>1</sup> and Paul R. Holland<sup>1</sup>

<sup>1</sup>British Antarctic Survey, High Cross, Madingley Road, Cambridge CB3 0ET, UK and <sup>2</sup>Department of Geography and Environmental Sciences, Northumbria University, Newcastle upon Tyne, UK

**Abstract**

Sea level rise contributions from the Pine Island Glacier (PIG) are strongly modulated by the backstress that its floating extension – Pine Island Ice Shelf (PIIS) – exerts on the adjoining grounded ice. The front of PIIS has recently retreated significantly via calving, and satellite and theoretical analyses have suggested further retreat is inevitable. As well as inducing an instantaneous increase in ice flow, retreat of the PIIS front may result in increased ocean melting, by relaxing the topographic barrier to warm ocean water that is currently provided by a prominent seabed ridge. Recently published research (Bradley and others, 2022a) has shown that PIIS may exhibit a strong melting response to calving, with melting close to the PIG grounding line always increasing with ice front retreat. Here, we summarise this research and, additionally, place the results in a glaciological context by comparing the impact of melt-induced and ice-dynamical changes in the ice shelf thinning rate. We find that while PIG is expected to experience rapid acceleration in response to further ice front retreat, the mean instantaneous thinning response is set primarily by changes in melting, rather than ice dynamics. Overall, further ice front retreat is expected to lead to enhanced ice-shelf thinning, with potentially detrimental consequences for ice shelf stability.

**Introduction**

The Antarctic Ice Sheet mainly contributes to sea level rise (SLR) via increases in ice flow from its grounded regions into adjoining floating ice shelves, across grounding lines. Ice sheet flow, and thus SLR contributions, are often strongly modulated by ice shelves via the backstress (or ‘buttressing’) they exert on the grounded ice (Gudmundsson and others, 2019).

How much buttressing a particular ice shelf exerts depends on the specific glacier characteristics. PIG, in West Antarctica, which is currently Antarctica’s largest contributor to SLR (IMBIE, 2018), is an example of a glacier whose flow is strongly influenced by its ice shelf. PIG has accelerated significantly over the satellite era: in 2013, its trunk was flowing approximately twice as fast (4 km/yr) as in the mid-1970s (2 km/yr) (Mouginot and others, 2014); this acceleration is understood to have resulted from a loss of buttressing following both melt-driven ice shelf thinning (e.g. Favier and others, 2014) and large scale calving (De Rydt and others, 2021). The large (approximately 12%) speed-up of PIIS in 2020, however, is thought to have resulted solely from the ice-dynamic response to reduced ice shelf buttressing following an ice front retreat of approximately 19 km in early 2020 (Joughin and others, 2021), with melt driven thinning not playing an important role.

In addition to significant recent retreat, further ice front retreat of PIIS appears highly likely: the recent calving of PIIS was coincident with a rapid increase in ice shelf damage (Lhermitte and others, 2020), which is thought to have preconditioned the shelf for further calving. Furthermore, ice front retreat may promote further calving via a damage-calving feedback loop (Sun and others, 2017) in which ice front retreat reduces buttressing, leading to ice acceleration, enhanced shear stresses, increased ice damage and ultimately further calving (Fig. 1).

**Melt response to PIIS calving**

As well as an ice dynamic response, there may be changes to melt rates on PIIS following ice front retreat. This is because the topographic blocking by the combination of a seabed ridge beneath PIIS and the ice shelf itself reduces the amount of relatively warm Circumpolar Deep Water able to reach the cavity inshore of the ridge, thereby restricting the amount of melting that can take place (Dutrieux and others, 2014; De Rydt and others, 2014). Ice front retreat might relax this topographic barrier and thus result in altered melt rates on PIIS.

To investigate this possibility, Bradley and others (2022a) performed numerical experiments in which they explicitly resolved the ocean cavity circulation and ice shelf melting using the MITgcm (Marshall and others, 1997) in a geometry accurately resembling PIG. A full description of the model setup, experiments, and results can be found in Bradley and others (2022a). Six experiments were performed in total, each featuring a different ice front position (Fig. 2a), while the grounding line position and ice thickness in areas of shelf not removed were fixed. Comparing melt rates between experiments with different ice front



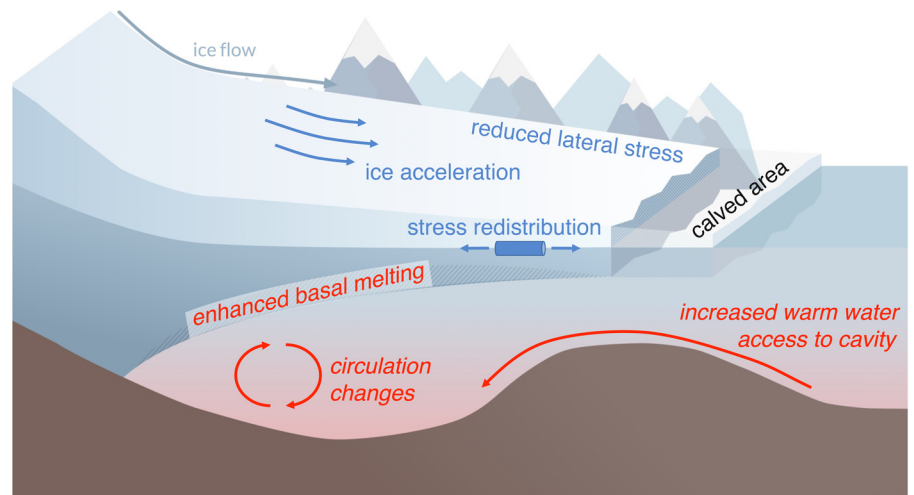


**Figure 1.** Which processes occur in the instantaneous response of PIIS to ice front retreat? Red (also italic) and blue labels indicate ocean and ice-dynamic processes which might result from ice front retreat, respectively; ultimately, these processes result in reduced ice shelf buttressing.

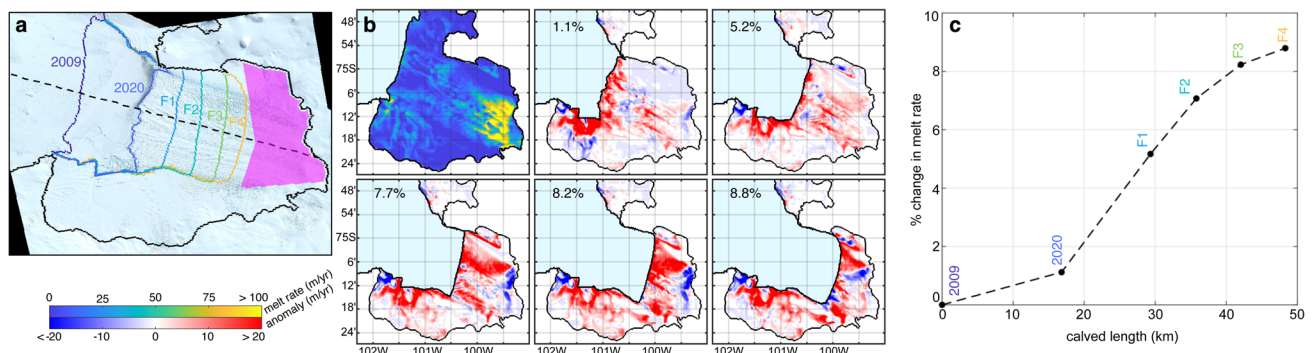


**Figure 2.** (a) Ice front positions used in experiments designed to assess the melt response of the PIIS to calving. Each experiment corresponds to a different ice front position as labelled: ice fronts labelled 2009 and 2020 indicate the ice front position in those years, while ice fronts labelled F1–F4 correspond to hypothetical future ice front positions. The solid black line indicates the 2009 grounding line from Joughin and others (2010). The dashed line roughly indicates the centreline of the cavity, along which the calved length – the difference between the ice front in the respective experiments and the 2009 ice front – is measured. Mean melt rate values shown in (c) are calculated over the shaded pink region. The background image is a Sentinel 2 mosaic from November 2020. (b) Simulated melt rate in the 2009 Pine Island geometry (first panel) and cumulative (i.e. measured to the first panel) melt rate anomalies (other panels). (c) Percentage enhancement in melt rate as a function of calved length measured relative to the 2009 geometry. Values correspond to those shown as text labels in (b).

positions offers insight into the melt response to calving: Bradley and others, 2022a found that, while the maps of melt rate display complex patterns of change upon ice front retreat (Fig. 2b), the mean melt rate close to the PIIS grounding line increases monotonically with retreat (Fig. 2c). This means that, assuming that nothing else about the geometry changes, ice front retreat always enhances melting. This enhancement results from both an increase in the amount, and temperature, of relatively warm water crossing the seabed ridge, as well as changes in the cavity circulation following ice front retreat (Fig. 1) (Bradley and others, 2022a).

### Ice dynamic response to PIIS calving

In addition to changes in basal melting, calving causes the ice sheet to adjust mechanically to the loss of a section of its restraining ice shelf. We refer to this as the ice-dynamic response. To facilitate a comparison between the melt and ice-dynamic responses to calving, we consider mass conservation:

$$\frac{\partial h}{\partial t} = -\dot{m} - \nabla \cdot (h\mathbf{u}). \quad (1)$$

Here  $h$  is the ice thickness,  $\mathbf{u}$  the depth-averaged ice velocity,  $\dot{m}$  the basal melt rate (positive indicates ice removal). Surface accumulation is small compared to melting on PIIS (e.g. Nakayama and others, 2022) and is therefore ignored.

Instantaneous adjustments to the rate of change ice thickness,  $\partial h/\partial t$ , consist of two components: changes in the melt rate (first term on the right hand side of (1)) and changes in the flux divergence (second term). Calving induces changes in both of these: changes in melting occur because of a dynamical adjustment in the ocean circulation, whereas changes in flux divergence occur because of a dynamical adjustment in the ice flow. Here, we compare these contributions by running a series of ice sheet model experiments and comparing the modelled flux divergence response to calving with the melt response described above. We note, however, that this is an inherently coupled system – a coupled ice-ocean model must be used to assess the transient response – and comment on this in the ‘Outlook’ section below.

To facilitate the comparison between melting and ice-dynamic contributions to changes in  $\partial h/\partial t$ , we used the Úa ice sheet model (Gudmundsson and others, 2019; Gudmundsson, 2022), with the setup as described by De Rydt and others (2021), to determine changes in ice velocity and flux divergence in response to changes in ice front position, according to those shown in Fig. 2a. Úa solves the vertically integrated formulation of the momentum equations on an unstructured mesh using the finite element method. Basal slipperiness and ice viscosity parameters were obtained using a commonly applied optimisation procedure, as described in detail by De Rydt and others (2021).

Figure 3e shows modelled ice velocity anomalies relative to the modelled 2009 ice velocity, which is shown in Fig. 3a. Upon

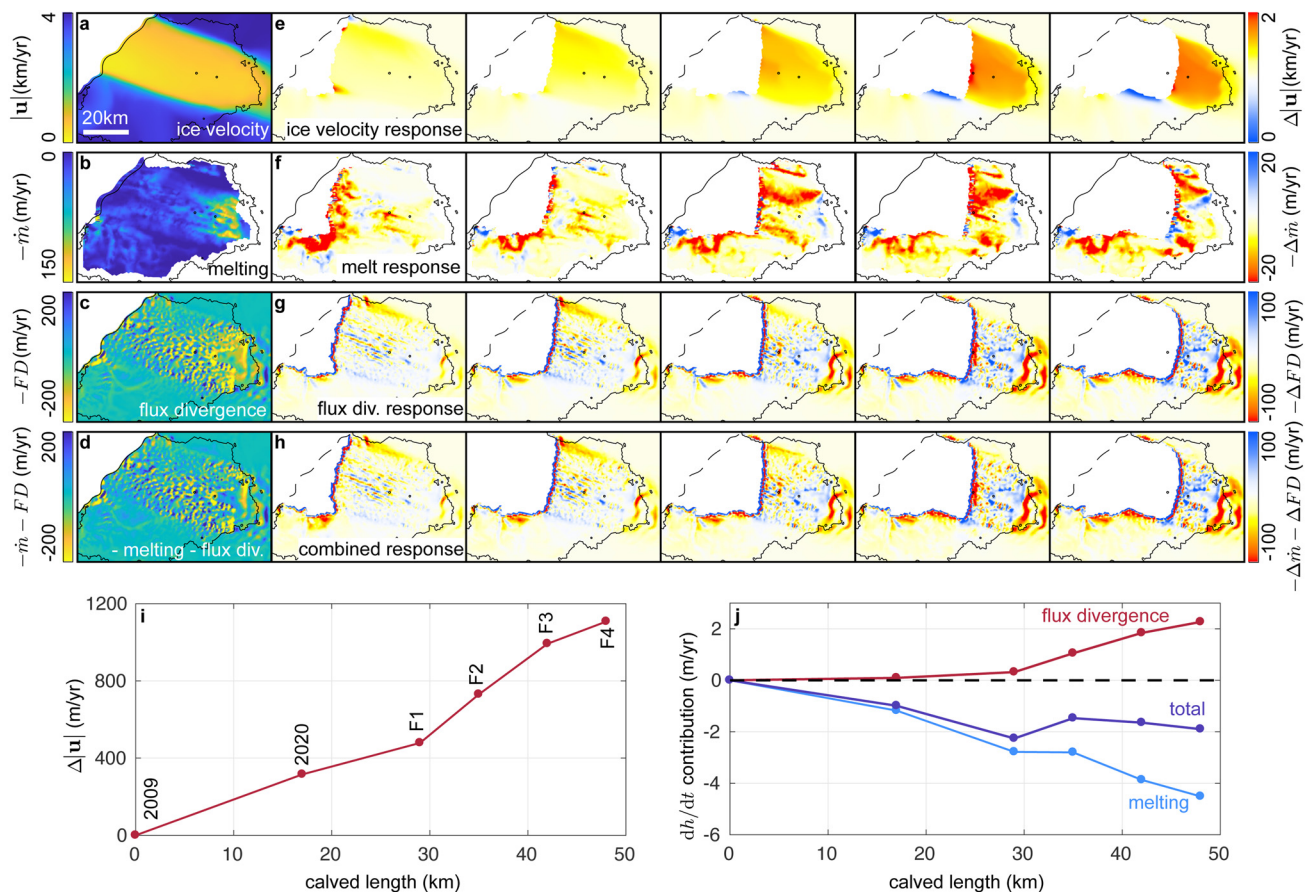


**Figure 3.** Comparison of the instantaneous ice dynamic and melt responses to PIIS ice front retreat. (a) Modelled PIG ice velocity and (e) velocity anomalies following ice front retreat (ice front retreat from left to right). (b)–(d) Negative basal melt rate  $-m$ , negative flux divergence  $-FD = -\nabla \cdot (hu)$ , and thinning rate  $-m - \nabla \cdot (hu)$  (i.e. the sum of (b) and (c)), alongside (f–h) responses following ice front retreat. Note the different colour bars in (f) and (g–h). (i) Mean velocity perturbation measured over the inner cavity (pink box in Fig. 2a), relative to the experiment with the 2009 ice front. (j) As in (i) but for the melt, flux divergence and total (sum of the melt and flux divergence) contributions. Note that the melt rates shown in (b) and (f) are as in Fig. 2b, but Fig. 2b uses a slightly different grounding line position (the grounding line shown here is from 2016 (De Rydt and others, 2021), while Fig. 2 shows a 2009 grounding line (Joughin and others, 2010)).

retreating the ice front from its 2009 position to its 2020 position, the mean ice velocity increases by approximately 400 m/yr (Fig. 3i), which is consistent with observations (Joughin and others, 2021). Further ice front retreat of PIIS is expected to induce significant further acceleration, with a velocity response that is approximately linear in the loss of ice shelf area (Fig. 3i): the model predicts an approximately 115 m/yr ice speed-up per 5 km length of ice shelf removed. (For context, the current retreat rate of the PIIS front is 5 km/yr (Joughin and others, 2021) and the mean (predominantly melt-driven) speed-up of PIIS between 1970 and 2010 was 40 m/yr<sup>2</sup>.) Note that this result is in contrast to a similar analysis applied to the Larsen C ice shelf (Mitcham and others, 2022), which indicated that progressive loss of ice shelf area results in a highly non-linear response of the grounding line flux, with the largest acceleration linked to loss of ice within 10 km of the grounding line. This emphasises the importance of the entire central portion of PIIS for buttressing of the PIG.

Figures 3b–d show, respectively, the negative melt rate, negative flux divergence, and their sum – the effective thinning rate – in the 2009 ice front experiment, alongside anomalies of these quantities in the calving scenarios (f–h, respectively). The large ice velocity response is also borne out in the flux divergence response, which is an order of magnitude larger than the corresponding melt response in many places (noting the different limits on the colour bars in Figs. 3f and g–h). Equivalently, the patterns of thinning rate anomalies (Fig. 3h) are highly similar to the patterns of flux divergence anomalies (Fig. 3g). Although the patterns of flux divergence anomalies are highly variable,

featuring regions of large positive and negative anomalies, the mean flux divergence response in the inner cavity region (the pink box in Fig. 2a) is positive and increasing with ice front retreat (Fig. 3j), indicating that flux divergence changes following ice front retreat always promote a more positive  $dh/dt$ . This is consistent with increased ice advection into the shelf concomitant with increased ice velocity. However, this positive net flux divergence contribution to the rate response is outweighed by the negative net melting contribution (Fig. 3j): our simulations suggest that the instantaneous response to PIIS calving is always *further thinning*. This highlights the crucial role that changes in melting following ice front retreat might play: without a change in melting following ice front retreat, the instantaneous response would promote ice shelf thickening (red line in Fig. 3j is positive); however, as a result of the changes in melting, we expect further ice shelf thinning following ice front retreat (purple line in Fig. 3j is negative).

## Outlook

Although the analysis included in this paper does not provide quantitative predictions of the transient evolution of PIIS following calving, the instantaneous analysis is highly informative. Most pertinently, it demonstrates the importance of calving on changes in PIIS buttressing and hence flow across the grounding line. We have shown that all areas of the PIIS are important for buttressing PIG, in contrast to many other regions of Antarctica in which only ice shelf areas close to grounding lines provide strong buttressing (Fürst and others, 2016). As well as this, the

instantaneous analysis demonstrates a large immediate PIIS velocity response to calving (on the same order of magnitude as changes over the past 10 years Mouginit and others, 2014), which would be expected to lead to significant changes on longer (decadal) timescales, as well as explicitly demonstrating that ice shelf melt rates may depend on ice front position, which no present day parametrization of melting accounts for (Bradley and others, 2022b). Finally, it demonstrates that the melt response to calving could enhance the impact of calving on the ice dynamics. We also note that satellite data (Joughin and others, 2021) suggests that the significant ice acceleration over the period 2017–2020 was synchronous with prolonged ice front retreat over the period, following a seven year period with little acceleration; this suggests that the immediate response to calving is comparable to, or may even dominate over, the background decadal trend in speed-up. However, a longer observational record is required to decompose responses on different timescales following such calving.

Due to the geometric feedbacks between melting, ice velocity, and calving shown above, investigating the post-instantaneous response of PIIS to ice front retreat in detail requires the use of a coupled ice-ocean model with a damage-calving scheme included (a ‘coupled ice-ocean-calving’ model). Coupled ice-ocean models have only recently begun to emerge (e.g. De Rydt and Gudmundsson, 2016; Seroussi and others, 2017; Favier and others, 2019; Smith and others, 2021), with most ice sheet projections still relying on parametrizations of melting (e.g. Bradley and others, 2022b), which are unable to capture the important feedbacks between calving and melting. The inclusion of calving schemes within ice sheet models is a nascent field, and, to the authors’ knowledge, there are no extant coupled ice-ocean-calving models. Since such models are not yet available, the instantaneous approach taken here remains the best option to assess the importance of calving for changes in ice-shelf buttressing and hence flow across the grounding line.

The potential imminence of PIIS’s decline, and understanding the implications of such, should provide urgent motivation to the modelling community to develop coupled models with moving ice fronts. There are, however, significant computational challenges to overcome before such models are ready (Asay-Davis and others, 2017). There is no uniform ‘grand-challenge’ here, rather individual models face specific difficulties. Initially a delicate treatment of boundary conditions (e.g. Albrecht and others, 2011) was adopted to deal with moving ice fronts, while more recently, a level set method has been adopted fairly widely (Bondzio and others, 2016). Moving boundaries are problematic for ocean models since new grid cells are opened, possibly instantaneously. It remains unclear how to robustly implement calving in ocean models (Asay-Davis and others, 2017); progress has, however, been made on similar problems relating to grounding lines (another moving boundary in ice-ocean models) either by including a porous fluid layer beneath the ice (Goldberg and others, 2018), or by interpolating quantities into new grid cells in a physically consistent way (De Rydt and Gudmundsson, 2016). Besides the ongoing development in the numerical implementation of moving ice fronts, the community must also improve and validate calving parametrizations, which describe where calving should occur based on other model diagnostics. Calving laws, including that which gives rise to the marine ice cliff instability (DeConto and Pollard, 2016), add significant uncertainty into future SLR projections (Edwards and others, 2019) but remain contested and largely unvalidated.

Despite our lack of transient simulations, we can speculate on the longer-term implications of the modelled PIIS response to ice front retreat. Firstly, we have shown that the average instantaneous response is further ice shelf thinning; since enhanced ice shelf thinning promotes further calving (Liu and others, 2015),

there is the potential for a retreat-melting feedback loop in which ice front retreat enhances melting, which in turn promotes enhanced calving and thus ice front retreat, potentially encouraging collapse of the PIIS. Ice shelf collapse might additionally be expedited by a retreat-damage feedback loop: the simulated ice acceleration that accompanies ice front retreat might enhance ice shelf damage (e.g. Sun and others, 2017) and thus precondition the shelf to calve further, leading to ice front retreat (e.g. Lhermitte and others, 2020). Finally, ice acceleration would be expected to be accompanied by thinning, which has the potential to alter the cavity geometry and influence the melt rate (Nakayama and others, 2022). In particular, thinning that further increases the gap between the seabed ridge and ice shelf might increase the flux of relatively warm water across the seabed ridge and thus increase melt rates close to the PIIS grounding line (De Rydt and others, 2014; Bradley and others, 2022a).

The recent acceleration and retreat of PIG is alarming and the possibility of the collapse of its restraining ice shelf now appears more likely than ever before. We have shown that future ice shelf front retreat is expected to lead to significant acceleration of the adjoining grounded ice, which might additionally promote further calving via a damage-acceleration-calving feedback loop. The acceleration of the grounded ice may be exacerbated by an increase in ice shelf melting in response to ice front retreat, with this melt response promoting further thinning and calving. An extreme acceleration of PIG, as suggested by our simulations, would undoubtedly have significant consequences for future SLR contributions from the entire WAIS, which operates as a connected system of glaciers together holding approximately 5.3 m of SLR equivalent of ice (Morlighem and others, 2020). Given the possibility of significant near-future acceleration of PIG, a research priority must be to better understand the response of the entire WAIS to abrupt acceleration of its constituent glaciers. More generally, such acceleration and possible collapse represents an extreme scenario with far-reaching consequences; the implications of such high consequence events warrants a significant research effort, particularly as their likelihood is expected to increase in a warming world.

## References

- Albrecht T, Martin M, Haseloff M, Winkelmann R and Levermann A (2011) Parameterization for subgrid-scale motion of ice-shelf calving fronts. *The Cryosphere* 5(1), 35–44.
- Asay-Davis XS, Jourdain NC and Nakayama Y (2017) Developments in simulating and parameterizing interactions between the southern ocean and the Antarctic ice sheet. *Current Climate Change Reports* 3(4), 316–329.
- Bondzio JH, and 6 others (2016) Modelling calving front dynamics using a level-set method: application to Jakobshavn Isbræ, West Greenland. *The Cryosphere* 10(2), 497–510.
- Bradley AT, Bett DT, Dutrieux P, De Rydt J and Holland PR (2022a) The influence of Pine Island Ice Shelf calving on basal melting. *Journal of Geophysical Research Oceans* 127(9), e2022JC018621.
- Bradley AT, Rosie Williams C, Jenkins A and Arthern R (2022b) Asymptotic analysis of subglacial plumes in stratified environments. *Proceedings of the Royal Society A* 478(2259), 20210846.
- DeConto RM and Pollard D (2016) Contribution of Antarctica to past and future sea-level rise. *Nature* 531(7596), 591–597.
- De Rydt J and Gudmundsson GH (2016) Coupled ice shelf-ocean modeling and complex grounding line retreat from a seabed ridge. *Journal of Geophysical Research: Earth Surface* 121(5), 865–880.
- De Rydt J, Holland PR, Dutrieux P and Jenkins A (2014) Geometric and oceanographic controls on melting beneath Pine Island glacier. *Journal of Geophysical Research: Oceans* 119(4), 2420–2438.
- De Rydt J, Reese R, Paolo FS and Gudmundsson GH (2021) Drivers of Pine Island glacier speed-up between 1996 and 2016. *Cryosphere* 15(1), 113–132.
- Dutrieux P, and 9 others (2014) Strong sensitivity of Pine Island ice-shelf melting to climatic variability. *Science* 343(6167), 174–178.

- Edwards TL, and 9 others** (2019) Revisiting Antarctic ice loss due to marine ice-cliff instability. *Nature* **566**(7742), 58–64.
- Favier L, and 8 others** (2014) Retreat of Pine Island glacier controlled by marine ice-sheet instability. *Nature Climate Change* **4**(2), 117–121.
- Favier L, and 7 others** (2019) Assessment of sub-shelf melting parameterisations using the ocean–ice-sheet coupled model nemo (v3. 6)–elmer/ice (v8. 3). *Geoscientific Model Development* **12**(6), 2255–2283.
- Fürst JJ, and 6 others** (2016) The safety band of Antarctic ice shelves. *Nature Climate Change* **6**(5), 479–482.
- Goldberg D, and 7 others** (2018) Representing grounding line migration in synchronous coupling between a marine ice sheet model and a z-coordinate ocean model. *Ocean Modelling* **125**, 45–60.
- Gudmundsson GH** (2022) Ghilmarg/uasource: An ice-flow model written in matlab, accessed 12-01-2023.
- Gudmundsson GH, Paolo FS, Adusumilli S and Fricker HA** (2019) Instantaneous Antarctic ice sheet mass loss driven by thinning ice shelves. *Geophysical Research Letters* **46**(23), 13903–13909.
- IMBIE** (2018) Mass balance of the Antarctic ice sheet from 1992 to 2017. *Nature* **558**(7709), 219–222.
- Joughin I, Shapero D, Smith B, Dutrieux P and Barham M** (2021) Ice-shelf retreat drives recent Pine Island glacier speedup. *Science Advances* **7**(24), eabg3080.
- Joughin I, Smith BE and Holland DM** (2010) Sensitivity of 21st century sea level to ocean-induced thinning of Pine Island glacier, Antarctica. *Geophysical Research Letters* **37**(20), L20502.
- Lhermitte S, and 7 others** (2020) Damage accelerates ice shelf instability and mass loss in Amundsen sea embayment. *Proceedings of the National Academy of Sciences* **117**(40), 24735–24741.
- Liu Y, and 7 others** (2015) Ocean-driven thinning enhances iceberg calving and retreat of Antarctic ice shelves. *Proceedings of the National Academy of Sciences* **112**(11), 3263–3268.
- Marshall J, Hill C, Perelman L and Adcroft A** (1997) Hydrostatic, quasi-hydrostatic, and nonhydrostatic ocean modeling. *Journal of Geophysical Research: Oceans* **102**(C3), 5733–5752.
- Mitcham T, Gudmundsson GH and Bamber JL** (2022) The instantaneous impact of calving and thinning on the Larsen c ice shelf. *The Cryosphere* **16**(3), 883–901.
- Morlighem M, and 9 others** (2020) Deep glacial troughs and stabilizing ridges unveiled beneath the margins of the Antarctic ice sheet. *Nature Geoscience* **13**(2), 132–137.
- Mouginot J, Rignot E and Scheuchl B** (2014) Sustained increase in ice discharge from the Amundsen sea embayment, West Antarctica, from 1973 to 2013. *Geophysical Research Letters* **41**(5), 1576–1584.
- Nakayama Y, Hirata T, Goldberg D and Greene CA** (2022) What determines the shape of a pine-island-like ice shelf?. *Geophysical Research Letters* **49**(22), e2022GL101272.
- Seroussi H, and 6 others** (2017) Continued retreat of Thwaites glacier, West Antarctica, controlled by bed topography and ocean circulation. *Geophysical Research Letters* **44**(12), 6191–6199.
- Smith RS, and 9 others** (2021) Coupling the UK earth system model to dynamic models of the Greenland and Antarctic ice sheets. *Journal of Advances in Modeling Earth Systems* **13**(10), e2021MS002520.
- Sun S, Cornford SL, Moore JC, Gladstone R and Zhao L** (2017) Ice shelf fracture parameterization in an ice sheet model. *The Cryosphere* **11**(6), 2543–2554.